

# Heat Losses of Fire Gases in a Mine Drift with Rough Rock Surface and Forced Longitudinal Ventilation

Rickard Hansen

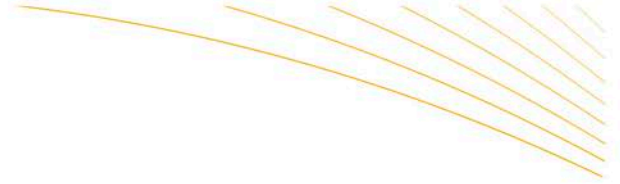




## Table of contents

---

<b>Abstract</b> .....	<b>3</b>
<b>Nomenclature</b> .....	<b>4</b>
<b>1. Introduction</b> .....	<b>6</b>
<b>2. Spread of fire gases and heat losses with respect to a rough mine drift surface</b> .....	<b>9</b>
2.1 The spread of fire gases in a mine drift.....	9
2.2 Boundary conditions, solid/gas interface.....	10
2.3 Convective heat transfer coefficient.....	12
2.4 Radiation term.....	14
<b>3. Conducted full-scale experiments</b> .....	<b>18</b>
3.1 Surface roughness measurements.....	18
<b>4. Three-dimensional analysis</b> .....	<b>20</b>
<b>5. Results of experiments and three-dimensional analysis</b> .....	<b>23</b>
5.1 Drilling rig fire.....	23
5.2 Loader fire.....	26
<b>6. Discussion</b> .....	<b>30</b>
<b>7. Conclusions</b> .....	<b>34</b>
<b>8. References</b> .....	<b>35</b>



## Abstract

---

The influence on the fire gases temperature with respect to the surface roughness in a mine drift is investigated. A number of correlations are investigated and compared with experimental results from full-scale fire experiments. During the analysis it is found that an expression by Nunner results in predicted average fire gas temperatures closest to the measured temperatures of the two experiments. The other correlations are found to significantly over predict the average fire gas temperature. During the occurrence of backlayering the correlation by Nunner is found to predict much higher temperatures. When subtracting the energy lost to backlayering, the resulting calculated temperature curve is found to fit the measured values very well. When calculating the average fire gas temperature, a key factor is determined with respect to the smoke spread in a mine drift as well as the risk of fire spread.



## Nomenclature

---

$A_{flames}$  = flame area ( $m^2$ )

$AH_w$  = absolute humidity of air ( $kg/m^3$ )

$AH_{ww}$  = absolute humidity near wet wall ( $kg/m^3$ )

$a$  = side length of mine drift cross section (m)

$b$  = side length of mine drift cross section (m)

$C$  = correction factor

$c_p$  = specific heat capacity of the fluid at constant pressure (J/kg·K)

$c_{p,s}$  = specific heat capacity of solid at constant pressure (J/kg·K)

$D$  = diameter of tunnel or mine drift (m)

$D_h$  = hydraulic diameter of the tunnel or mine drift (m)

$D_t$  = mass transfer coefficient

$E$  = emissive power ( $kW/m^2$ )

$f$  = Darcy friction factor

$F$  = view factor

$F_{roughness}$  = roughness factor

$Fr$  = Froude number

$H$  = height of mine drift (m)

$h$  = height (m)

$h_{total}$  = total heat transfer coefficient ( $W/m^2 \cdot K$ )

$h_c$  = convective heat transfer coefficient ( $kW/m^2 \cdot K$ )

$K$  = airway friction factor ( $kg/m^3$ )

$k$  = thermal conductivity ( $kW/m \cdot K$ )

$k_{air}$  = thermal conductivity of air ( $kW/m \cdot K$ )

$k_g$  = thermal conductivity of fire gases ( $kW/m \cdot K$ )

$k_w$  = thermal conductivity of wall ( $kW/m \cdot K$ )

$L$  = length of tunnel or mine drift (m)

$L_{water}$  = latent heat of evaporation (kJ/kg)

$\dot{m}_a$  = mass flow in tunnel or mine drift (kg/s)

$Nu$  = Nusselt number

$P$  = perimeter of tunnel or mine drift (m)

$Pr$  = Prandtl number

$\dot{Q}$  = heat release rate (kW)

$\dot{q}_{incident}''$  = incident heat flux ( $kW/m^2$ )

$\dot{q}_{rad}''$  = radiative heat flux ( $kW/m^2$ )

$R$  = coordinate in radial direction (m)

$r$  = radius (m)

$R_0$  = hydraulic radius of airway (m)

$Re$  = Reynolds number

$t$  = time (s)



$T_a$  = air temperature (K)

$T_{avg}$  = average gas temperature over the entire cross-section at a given position (K)

$\Delta T_{avg}$  = average gas temperature difference (K)

$\Delta T_{cf}$  = gas temperature difference between ceiling and floor (K)

$T_g$  = fire gas temperature (K)

$\Delta T_h$  = gas temperature rise above ambient at height  $h$  (K)

$T_m^i$  = node temperature at time step  $i$  (K)

$T_0$  = ambient temperature (K)

$T_w$  = wall temperature (K)

$T_\infty$  = free-stream temperature (K)

$u$  = fluid velocity (m/s)

$v$  = average fluid velocity (m/s)

$x$  = distance along the mine drift (m)

$\alpha$  = absorptivity factor

$\varepsilon$  = emissivity factor

$\varepsilon_{roughness}$  = roughness amplitude (m)

$\rho$  = fluid density ( $\text{kg/m}^3$ )

$\rho_s$  = solid density ( $\text{kg/m}^3$ )

$\sigma$  = Stefan-Boltzmann constant,  $5.67 \cdot 10^{-11} \text{ kW/m}^2 \cdot \text{K}^4$

$\tau$  = transmissivity factor

$\tau_{transport}$  = transport time (s)

$\psi$  = wetness (area ratio)



## 1. Introduction

---

The environment in a hard rock mine drift is distinguished by rough rock surfaces, where the surface roughness magnitude of the surrounding surfaces could be substantial. In the case of a fire in a mine drift the environment will affect the fire behaviour in numerous ways, such as the heat release rate of the fire and the heat losses of the streaming fire gases along the mine drift. An increasing surface roughness will increase the turbulence of the fire gases as well as the area of the surrounding rock surfaces which will result in an increasing heat transfer from the fire gases to the surrounding rock surfaces and a more rapidly decreasing fire gas temperature as opposed to a tunnel with smooth surfaces. This in turn will affect the behaviour and spread of the fire gases along the mine drift as well as the likelihood that a fuel package at a certain distance from the fire will ignite, initiating a second fire.

This paper focuses on and investigates the influence on the fire gases temperature with respect to the surface roughness in a mine drift with longitudinal ventilation and in the near vicinity of the fire. A number of correlations are investigated and the calculated values are compared with experimental values from earlier conducted full-scale fire experiments in a mine drift.

The comparison with experimental data was used in order to verify the output of the different correlations. The experimental data was obtained from full-scale experiments presented by Hansen and Ingason (2013). These tests were found to be very well defined and fit very well to the aim of the work presented here. The purpose of this paper is to provide knowledge on the smoke behaviour in a mine drift that could be applied when modelling the smoke spread, smoke control, fire spread, overall fire behaviour etc in an underground hard rock mine, where the spread of smoke is a major risk to the miners.

An earlier study show that better knowledge about smoke behaviour and fire spread is needed for underground hard rock mines (Hansen, 2015). A limited number of studies have been conducted on the heat exchange between rock and adjacent fluid in underground mines and tunnels. Most of the studies have focused on the heat exchange due to the humid environment but very few studies have dealt with the influence of the rough rock surface on the heat exchange. The numbers of studies in the field are very few, the studies do not penetrate the subject in-depth and obviously the subject has not been investigated to any larger extent.

Wolski (1995) conducted a study where the heat exchange between flowing air and tunnel walls was modeled. The model presented accounted for the heat loss due to convection and radiation. The convective heat transfer coefficient was calculated using an expression by Starfield and Dickson (1967) who in turn had added a friction factor to an existing expression by Rohsenow and Choi (1963) valid for smooth surfaces:

$$h_c = \frac{F_{roughness} \cdot k_{air} \cdot 0.023 \cdot Re^{0.8} \cdot Pr^{0.4}}{D} \quad (1)$$

The model was validated against model scale experiments and found to agree very well.

Dziurzynski, Tracz and Trutwin (1988) conducted simulations with a proposed mine fire model. In the model the fire was assumed to have a lumped character and only the convective heat transfer between the air and the rock was accounted for. It is unclear whether the surface roughness of the rock surfaces was accounted for in the model.

Chang and Greuer (1987) presented a paper that assumed circular airways with wood uniformly distributed over the entire airway walls. The heat transfer between the wall and the air was assumed to be composed of convective and radiative heat transfer components. The surface roughness of the wall surfaces was not considered in the heat transfer calculations, which is not surprising given that the walls were assumed to be covered by wood.

Simode (1985) presents a model to determine the smoke temperatures along mine drifts. Only the



convective heat transfer mechanism was included in the heat transfer calculations between the smoke and the wall. The surface roughness of the surfaces was not considered in the calculations of the convective heat transfer.

McPherson (1986) described a model where the overall heat transfer coefficient -  $h$  - at the surface of the airway is assumed to vary mainly with the air velocity and the roughness of the airway surface. An empirical expression by Scott (1958) was applied to calculate the overall heat transfer coefficient:

$$h_{total} = 3540 \cdot K \cdot v \quad (2)$$

Chang and Greuer (1985) set up the following initial boundary condition - accounting for the enthalpy change due to evaporation as well as the heat transfer from the mine air to the wall - for a section perpendicular to the airway axis:

$$R = R_0 \quad k_w \frac{\partial T_w}{\partial R} = h_c \cdot (T_w - T_a) + \psi \cdot L_{water} \cdot D_t \cdot (AH_{ww} - AH_w) \quad (3)$$

Beard et al. (2005) set forward the following expression for the average fire gas temperature over the entire cross-section at a given position along a tunnel with longitudinal ventilation:

$$T_{avg}(x, t) = T_0 + [T_{avg, x=0}(\tau) - T_0] \cdot e^{-\frac{h_{total} \cdot P \cdot x}{\dot{m}_a \cdot c_p}} \quad (4)$$

$$\tau_{transport} = t - \left( \frac{x}{u} \right) \quad (5)$$

$$T_{avg, x=0}(\tau_{transport}) = T_0 + \frac{2}{3} \frac{\dot{Q}(\tau)}{\dot{m}_a \cdot c_p} \quad (6)$$

The longitudinal ventilation velocity was assumed to be non-variant along the tunnel, a lumped heat transfer coefficient both for convective and radiative heat losses was assumed and the wall temperature was assumed to be equal to the ambient temperature. The roughness of the surfaces was not considered in the set of equations.

Newman and Tewarson (1983) presented the following equation for calculating the average convective heat transfer coefficient to the walls along a rectangular duct:

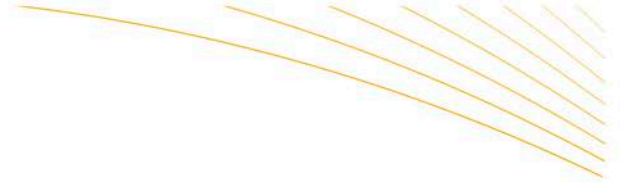
$$h_c = 0.026 \cdot \text{Re}_{D_h}^{-0.2} \cdot \left( 1 + \left( \frac{D_h}{x} \right)^{0.7} \right) \cdot \rho \cdot c_p \cdot v \quad (7)$$

The roughness of the surfaces was not considered in the equation.

In the following, the theory of fire gas behaviour, the convective and radiative heat transfer components in a mine drift with longitudinal ventilation are outlined and discussed. A model for calculating the heat losses of the fire gases in a mine drift is set up and investigated together with a number of correlations for calculating the convective heat transfer coefficient. The resulting average fire gas temperatures of the model are



compared to earlier results from full-scale fire experiments. Additional sensitivity analysis on selected parameters were performed and discussed.



## 2. Spread of fire gases and heat losses with respect to a rough mine drift surface

Given the forced flow conditions and the extensive length of a mine drift, the transition to turbulent flow will take place close to the leading edge and will apply for the major part of the mine drift. Due to the enclosed nature, geometrical appearance and extensive length of the mine drift, the duct flow case would be the most appropriate case for the mine drift. The focus will therefore be on turbulent duct flow in this paper.

### 2.1 The spread of fire gases in a mine drift

The fire gases in a mine drift will ascend and spread along the ventilation direction. The smoke spread is largely determined by the occurring smoke stratification, which in turn is depending upon the air velocity in the mine drift, the dimensions of the mine drift, the heat release rate as well as the distance to the fire. With a low or no forced air velocity the smoke stratification is high in the vicinity of the fire while at the other end – at high air velocities – the smoke stratification is low downstream from the fire. With increasing mine drift height and increasing distance to the fire, the vertical temperature gradients will decrease and thus also the smoke stratification. An increase in the heat release rate will result in an increase in the vertical temperature gradients and an increase in the smoke stratification. An example of stratification in a mine drift is shown in Figure 1.

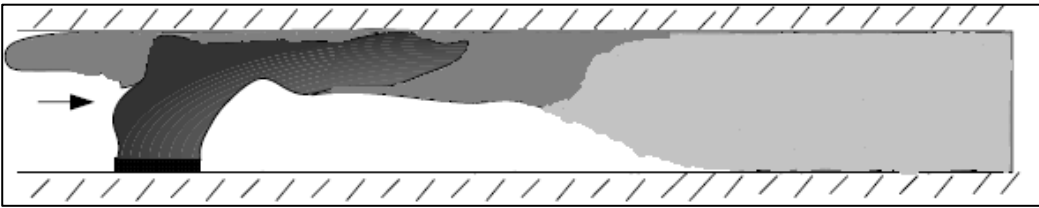


Figure 1. The stratification of fire gases in a mine drift

Newman (1984) presented a number of correlations for the temperature stratification in a duct fire using a Froude number correlation. Newman divided the duct into three different regions depending on the degree of stratification.

For region I - in the immediate and near vicinity of the fire - the gas temperature rise above ambient at height  $h$  -  $\Delta T_h$  - is equal to the difference between the gas temperature near the ceiling ( $h = 0.88 \cdot H$ ) and the gas temperature near the floor ( $h = 0.12 \cdot H$ ) -  $\Delta T_{cf}$ . The gas temperature near the floor is more or less at ambient temperatures and  $Fr \leq 0.9$ ,  $\Delta T_{cf} / \Delta T_{avg} > 1.7$ , describing a buoyancy dominating temperature stratification.

For region II we have the following conditions:  $0.9 < Fr < 10$ ,  $1.7 \geq \Delta T_{cf} / \Delta T_{avg} > 0.1$ , describing significant interaction of the ventilation velocity with the fire-induced buoyancy.

For region III we have:  $Fr \geq 10$ ,  $\Delta T_{cf} / \Delta T_{avg} \leq 0.1$  and stratification is insignificant resulting in the following relationship:  $\Delta T_h \approx \Delta T_{avg}$ .

The surface roughness will affect the stratification and smoke spread. An increasing surface roughness will lead to a decreasing stratification. Even though the effect of a rough surface was not specifically investigated by Newman (1984), an increasing surface roughness will increase the heat losses of the fire gases and decrease the ratio  $\Delta T_{cf} / \Delta T_{avg}$  and is therefore to some extent included in the correlation.



## 2.2 Boundary conditions, solid/gas interface

Downstream of the fire - providing that insignificant stratification prevails - the temperature gradient perpendicular to the flow direction will be near zero except for the region closest to the rock surface. Further upstream where the flow is not fully developed or where stratification prevails, the boundary layer will have a substantial influence on the heat transfer between the fluid and the rock surface. The influence of the boundary conditions on the heat transfer will have to be taken into account when examining the heat losses of the fire gases.

In the following the governing equations for the solid/gas interface for a surface exposed to radiant and convective heating are presented.

Wall temperature at the solid surface,  $t > 0$  :

$$T(0, t) = T_w \quad (8)$$

Boundary conditions at the boundary layer edge ( $y = \delta$ ),  $t > 0$  :

$$T(\delta, t) = T_\infty \quad (9)$$

$$\left. \frac{\partial T}{\partial y} \right|_{y=\delta} = 0 \quad (10)$$

Assuming:

- > Incompressible, steady flow.
- > Temperature change in the x-direction of the solid to be small and thus the conduction in the flow direction is negligible.

In the following, expressions for a laminar flow are presented and laid out as a starting point for the turbulent flow found in the mine drift of the two full-scale fire experiments. Taking advantage of the fact that the physical mechanism of heat transfer in turbulent flow is quite similar to that in laminar flow, a convective heat transfer coefficient - for turbulent conditions - will be applied in order to account for the turbulent flow.

Accounting for the heat radiation, and neglecting the viscous work and second-order differentials; the energy balance for an element inside the boundary layer can be expressed as:

$$\rho \cdot c_p \cdot \left( u \frac{\partial T}{\partial x} + v \frac{\partial T}{\partial y} \right) dx dy = k \frac{\partial^2 T}{\partial y^2} dx dy + \dot{q}_{rad}'' \quad (11)$$

The solid boundary condition at a plane on the rock surface is ( $y = 0$ ):



$$-kdx \frac{\partial T}{\partial y} \Big|_{y=0} = \rho \cdot c_p \cdot (v \cdot T) dx + \rho \cdot c_p \cdot \left( u \frac{\partial T}{\partial x} dx + T \frac{\partial u}{\partial x} dx \right) dy + \dot{q}_{rad}'' \Big|_{y=0} \quad (12)$$

Where:

$$\dot{q}_{rad}'' \Big|_{y=0} = \alpha \cdot \dot{q}_{incident}'' - \varepsilon \cdot \sigma \cdot (T_w^4 - T_g^4) \quad (13)$$

assuming radiant grey bodies.

The temperature gradient at the interface -  $\frac{\partial T}{\partial y} \Big|_{y=0}$  - will decrease with increasing thermal boundary layer thickness and thus also with an increasing horizontal distance.

The temperature continuity at the interface is expressed by the following equation:

$$T_g \Big|_{y=0} = T_w \Big|_{y=0} \quad (14)$$

Similarly for the heat flux continuity (no-slip condition):

$$k_w \frac{\partial T_w}{\partial y} \Big|_{y=0} = k_g \frac{\partial T_g}{\partial y} \Big|_{y=0} + \dot{q}_{rad}'' \Big|_{y=0} \quad (15)$$

In figure 2 the forced, steady flow case for a duct with flowing hot fluid can be seen with a control volume at the interface displaying the convective energy in and out of the control volume. The resulting second-order differentials of the convective energy were neglected in equation (12) above.

Due to the enclosed nature of a mine drift, the boundary layer will with increasing distance in the x-direction fill up the mine drift and the flow will become fully developed. The flow of fire gases in a longer mine drift will be fully developed for a considerable distance due to the geometrical appearance of the mine drift (i.e. the length of the mine drift is much larger than the diameter of the drift). Condition for a fully developed turbulent flow:

$$\left( \frac{x}{D} \right) \geq 10 \quad (16)$$

In the fully developed region the mean temperature of the hot fluid is decreasing in the x-direction, the vertical temperature gradient becomes more or less constant, and the convective heat transfer coefficient will



become independent of the position in the x-direction (still the coefficient will vary due to the influence of the surface roughness).

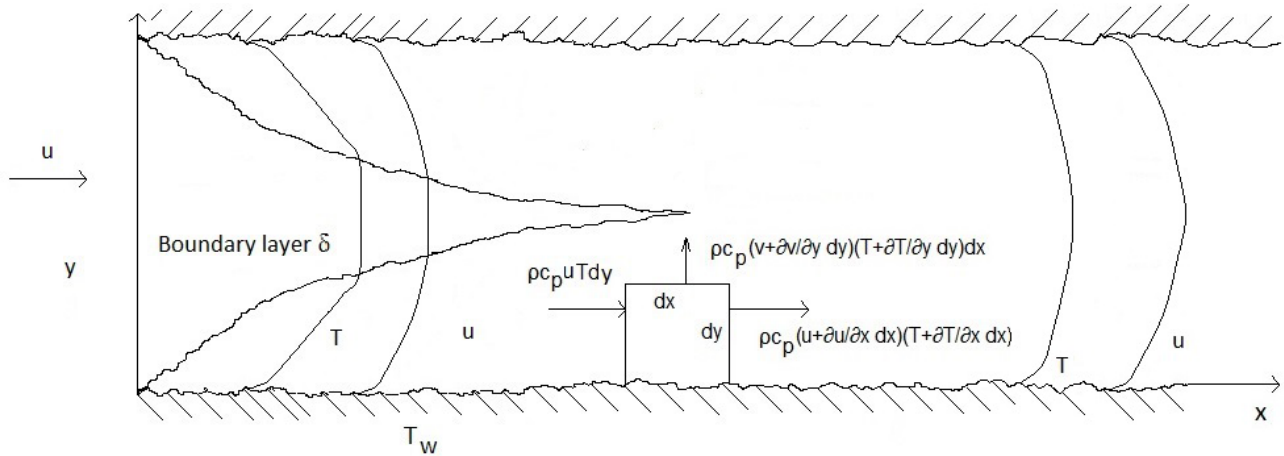


Figure 2. Forced, steady flow case for a duct with surface roughness features. For simplification the two boundary layers (thermal and hydrodynamic) was depicted having the same thickness and appearance

Simplifying the gas phase details - applying a convective heat transfer coefficient - equation (12) becomes:

$$-k \frac{\partial T}{\partial y} \Big|_{y=0} = h_c \cdot (T_g - T_w) + \dot{q}_{rad} \Big|_{y=0} \quad (17)$$

### 2.3 Convective heat transfer coefficient

The heat flux equation above (equation (17)) assumes laminar flow. The flow in the mine drift will generally - due to the forced ventilation - be turbulent. The influence of the turbulent flow will be accounted for by the convective heat transfer coefficient and thus relying on empirical expressions.

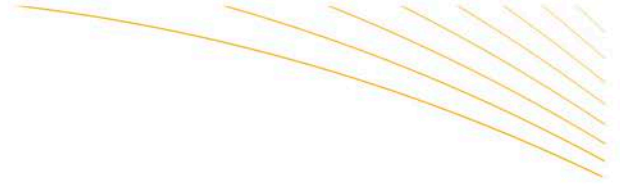
For a rough surface the laminar viscous sublayer will be broken up, resulting in a dramatic decrease in the conductive resistance of the sublayer. The convective heat transfer coefficient for a rough surface can therefore be much larger than for a smooth surface for the same flow conditions.

The convective heat transfer coefficient will vary with the surface roughness features. As the surface roughness features will have a random nature along the rock surface, a lumped/average value of the coefficient would be the most convenient and practical solution when calculating the heat losses of the fire gases.

Applying the Nusselt number expression when calculating the convective heat transfer coefficient:

$$Nu_L = \frac{h_c \cdot L}{k} \quad (18)$$

The Nusselt number expression can be used when fulfilling the following condition (Norris, 1970):



$$\frac{f}{f_{smooth}} \leq 4 \quad (19)$$

The friction factors in the correlations above and below were obtained from a Moody diagram.

Turbulent duct flow for circular ducts has been extensively explored, which is not the case for rectangular ducts. Still the results for circular ducts can be applied for rectangular ducts as well with fairly accurate results, applying a hydraulic diameter (Bhatti and Shah, 1987) as the characteristic length:

$$D_h = \frac{2 \cdot a \cdot b}{a + b} \quad (20)$$

Given that the cross section of a mine drift will generally have rounded edges and thus a mix of a rectangular and circular appearance, increasing the applicability of the hydraulic diameter.

A number of expressions for the Nusselt number - valid for fully developed turbulent duct flow, with a rough duct surface - are described below and were applied in the ensuing analysis.

Martinelli (1947) presented the following correlation:

$$Nu_{D_h} = \frac{Re_{D_h} \cdot Pr \cdot \sqrt{\frac{f}{2}}}{5 \cdot \left[ Pr + \ln(1 + 5 \cdot Pr) + 0.5 \cdot \ln \left( \frac{Re_{D_h} \cdot \sqrt{\frac{f}{2}}}{60} \right) \right]} \quad (21)$$

A correlation valid for  $Pr \approx 0.7$  was given by Nunner (1956):

$$Nu_{D_h} = \frac{Re_{D_h} \cdot Pr \cdot \left( \frac{f}{2} \right)}{1 + 1.5 \cdot Re_{D_h}^{\frac{1}{8}} \cdot Pr^{-\frac{1}{6}} \cdot \left[ Pr \cdot \left( \frac{f}{f_{smooth}} \right) - 1 \right]} \quad (22)$$

Bhatti and Shah (1987) presented the following correlation:



$$Nu_{D_h} = \frac{\left( Re_{D_h} \cdot Pr \cdot \left( \frac{f}{2} \right) \right)}{1 + \sqrt{\frac{f}{2}} \cdot (4.5 \cdot Re_{\epsilon}^{0.2} \cdot Pr^{0.5} - 8.48)} \quad (23)$$

The correlation is valid for  $0.5 < Pr < 10$ ,  $0.002 < \frac{\epsilon_{roughness}}{D_h} < 0.05$ , and  $Re > 1 \cdot 10^4$ .

A correlation by Bhatti and Shah (1987), which is valid for  $Re > 2300$ :

$$Nu_{D_h} = \frac{(f/2) \cdot (Re_{D_h} - 1000) \cdot Pr}{1 + \sqrt{\frac{f}{2}} \cdot [Re_{\epsilon_{roughness}}^{0.5} \cdot (17.42 - 13.77 \cdot Pr_t^{0.8}) - 8.48]} \quad (24)$$

where:

$$Pr_t = 1.01 - 0.09 \cdot Pr^{0.36} \quad \text{for } 1 \leq Pr \leq 145 \quad (25)$$

The parameters in the correlations above were evaluated at a mean temperature of the fluid, calculated at the cross-section of interest perpendicular to the mine drift axis.

In the entry section of a duct or in a section with stratification, the vertical temperature gradient will not be constant, and the convective heat transfer coefficient will not be independent of the position in the direction of the flow. In this section the Nusselt number will be larger than for the fully developed case. In the case of a mine drift it could be assumed in most cases that the thermal conditions will develop with a fully developed velocity profile being present, as the position of for example the fan will be further upstream of the fire. This case is classified as having a thermal entry region (Incropera et al., 2007) and the average Nusselt number for the entry region may be calculated applying the following correlation (Mills, 1962):

$$\frac{\overline{Nu}_{D_h,entry}}{Nu_{D_h}} = 1 + \frac{0.9756}{\left( \frac{x}{D_h} \right)^{0.760}} \quad (26)$$

## 2.4 Radiation term

A mine drift surface will be exposed to several radiation interchange terms: incident heat flux from the flames, incident heat flux from the fire gases and re-radiation from the rock surface to the surroundings. The



radiative heat flux term in equation (17) above describes the net radiative interchange for the rock surface. The term can be further evolved:

$$\begin{aligned} \dot{q}_{rad} \Big|_{y=0} = & \alpha_{RockSurface} \cdot E_{FireGases} \cdot F_{FireGases-RockSurface} \cdot \varepsilon_{FireGases} + \\ & \alpha_{RockSurface} \cdot E_{Flames} \cdot F_{Flames-RockSurface} \cdot \tau_{FireGasLayer} \cdot \varepsilon_{Flames} \\ & - \varepsilon_{RockSurface} \cdot E_{RockSurface} \cdot F_{RockSurface-FireGases} \end{aligned} \quad (27)$$

The emissive power of the fire gases-  $E_{FireGases}$  - is expressed by:

$$E_{FireGases} = \sigma \cdot T_g^4 \quad (28)$$

The view factor of the fire gases to the rock surface and vice versa -  $F_{FireGases-RockSurface}$  - could be assumed to be unity as the rock surface will be in direct contact and engulfed by the fire gases.

The emissivity of the fire gases will depend on the composition of the gases, wavelength, partial pressure and temperature. Simplifying by applying the gray gas assumption, the fire gas emissivity is calculated using:

$$\varepsilon_{FireGases} = C_{CO_2} \cdot \varepsilon_{CO_2} + C_{H_2O} \cdot \varepsilon_{H_2O} - \Delta \varepsilon_{CO_2-H_2O} \quad (29)$$

The correction factors were set to unity in the ensuing calculations and the emissivity factors were extracted from Hottel charts (Hottel, 1954), based upon measurements from full-scale fire experiments (Hansen and Ingason, 2013) and mean beam lengths assuming the shape of a partial cylinder - depending on the fire gas layer height - in the mine drift due to stratification.

The emissive power -  $E_{Flames}$  - of the flames is expressed by:

$$E_{Flames} = \frac{\dot{Q}_{rad}}{A_{flames}} \quad (30)$$

The radiative fraction of the total heat release rate may be assumed at 1/3 based upon the findings of earlier full-scale fire experiments in a copper mine (Ingason et al., 1994).

In the ensuing calculations the flame area was set equal to the width of the fire object multiplied with the flame height. The flame height was calculated using a correlation of Ingason and Li (2010) found to be the most appropriate correlation with respect to conducted full-scale mining fire experiments (Hansen, 2015).

The view factor of the flames to the rock surface -  $F_{Flames-RockSurface}$  - will be influenced by the rough rock surface. Protruding surface segments will have a larger view factor compared with a smooth surface segment. But on the back side of a protruding structure, the view factor will be less than for a smooth surface



segment. It is assumed in this paper that the higher view factors of protruding surfaces facing the flames will be cancelled out by the lower view factors of back side surfaces and thus a smooth surface is applied in the calculations.

The view factor between the flames and the different rock surface segments along the mine drift - assuming a circular mine drift - may be calculated using the following expressions between a flame element and the inner surface of a coaxial circular cylinder (Chung and Sumitra, 1972):

$$F_{d1-2} = \frac{1}{1 + \left(\frac{r}{x}\right)^2} - \frac{\left(1 - \frac{h}{x}\right)^2}{\left(1 - \frac{h}{x}\right)^2 + \left(\frac{r}{x}\right)^2} \quad \text{for: } \frac{h}{x} < 1 \quad (31)$$

$$F_{d1-2} = \frac{1}{1 + \left(\frac{r}{x}\right)^2} \quad \text{for: } \frac{h}{x} \geq 1 \quad (32)$$

The calculated mean flame height of the full-scale fire experiments was approximately mid-height of the mine drift, which is the same height of the coaxial flame element. Figure 3 displays the different parameters found in equations (31-32) above.

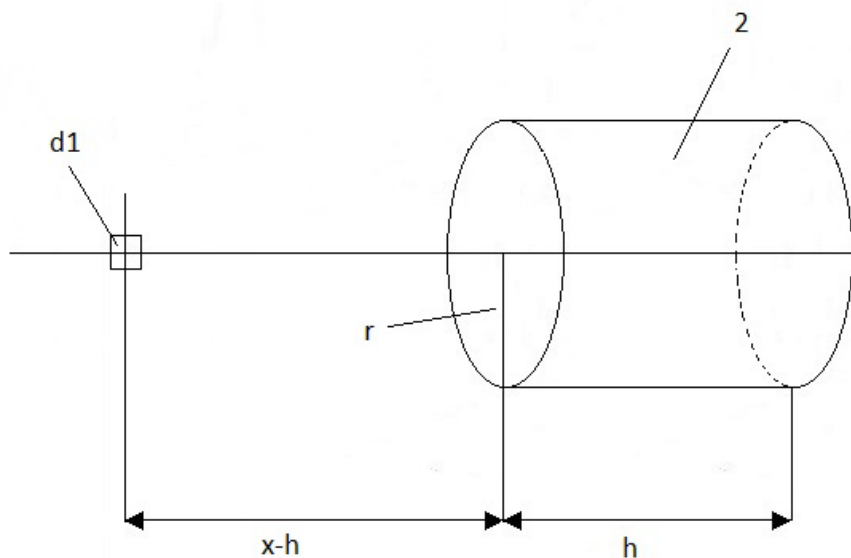
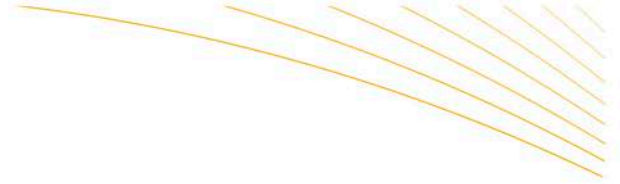


Figure 3. View factor parameters for a flame element to the inner surface of coaxial circular cylinder

The emissivity of the flames was set to unity in the ensuing calculations, assuming a black body.

Assuming that the fire gas layer is non-reflecting, the transmissivity of the fire gas layer is:



$$\tau_{FireGasLayer} = 1 - \varepsilon_{FireGases} \quad (33)$$

Fulfilling Kirchoff's law - since there is no angular dependence - the absorptivity of the rock surface is set equal to the rock surface emissivity.

The absorptivity of the rock surface was assumed at 0.41 in the ensuing analysis, which is applicable for Dolomite lime (Wilson, 2004) at 20°C.



### 3. Conducted full-scale experiments

---

Two full-scale fire experiments on mining vehicles were conducted in an underground dolomite mine in Sweden. The full-scale fire experiments involved a loader and a drilling rig and were conducted in order to provide much needed data for future fire safety designs in underground mines. The fire gas temperature was measured at certain heights at a measuring station, which was positioned ~35 m downstream of the loader fire and ~50 m downstream of the drilling rig fire. One of the reasons why the temperature was measured at different heights was to obtain the average temperature of the cross section at the measuring station. Besides the fire gas temperature, the ventilation velocity and gas concentrations were also measured at the measuring station primarily to obtain data for calculating the heat release rate of the fire. Approximate dimensions of the mine drift were 6x8 meter (HxW) and there were practically no differences in height between the fire and the measuring station. The actual shape of the mine drift was semi circular (or a rectangle with rounded edges), but the shape was assumed to be circular in the ensuing calculations.

All the fire gases were ventilated through the mine drift using a mobile fan in order to obtain the forced flow. The mobile fan was a Tempest fan model MGV L125, diesel powered, a diameter of 1.25 m and with a capacity of 217.000 m<sup>3</sup>/h. The fan was positioned ~110 m upstream of the drilling rig fire and ~125 m upstream of the loader fire. If setting the position of the fan as equivalent to the inlet and given that

$\left(\frac{x}{D_h}\right) \geq 10$  for both cases, a fully developed turbulent flow could be expected at the two fires. But when

looking into the stratification in the mine drift it was found that the entire section from the fires to the measuring station was within region I with distinct stratification. Thus the vertical temperature gradient would not be more or less constant and the stratification will have to be accounted for when calculating the Nusselt number.

See paper by Hansen and Ingason (2013) for further details on the experiments.

#### 3.1 Surface roughness measurements

Surface roughness can be distinguished by the random nature of the surface roughness structures and be found in two dimensions. Given that the amplitude of the surface roughness will have a decisive impact on the viscous sublayer and therefore also on the heat transfer to the rock surface, the roughness structures are described by the roughness amplitude in this paper. Due to the random nature of the structures an average value of the roughness amplitude is best suited when characterizing the roughness parameter:

$$\varepsilon_{roughness} = \frac{1}{n} \sum_{i=1}^n |x_i| \quad (34)$$

The width of the mine drift - where the full scale fire experiments took place - was measured at a number of places in order to get a measure on the roughness amplitude. Applying equation (34) above it was found that for the ten randomly chosen measuring points the roughness amplitude was approximately 0.1 m.

Roughness data on 54 mine drift sections were provided by LKAB Mining Corporation in order to investigate whether the calculated value above was a typical roughness value for a mine drift. The average roughness amplitude for the mine drift sections was calculated to approximately 0.11 m, thus very close to the calculated value.

Applying the roughness parameter, the relative roughness was calculated using the hydraulic diameter of the mine drift as the characteristic length.



Applying a Reynolds number of  $0.7 \cdot 10^6$  (corresponding to ventilation velocity of 2 m/s and a kinematic viscosity of air taken at 350 K) and a roughness amplitude of 0.1 m, it was found that the Nusselt number condition (equation (19)) was fulfilled for the mine drift of the full scale fire experiments.



## 4. Three-dimensional analysis

---

A model was set up in order to calculate the average fire gas temperature at the measuring station for the two full-scale fire experiments, applying the various listed correlations above. A quasi-steady process was applied in the model as a transient heat flux is faced and most equations for calculation of the surface temperature assume a constant heat flux. The quasi-steady process implies using a numerical method where at any instance in time the surface temperature can be described as if the surface was exposed to a steady state situation.

A time increment of 1 second was applied in the calculations and the mine drifts of the experiments were divided into a number of segments in the axial direction with a width of 0.5 m.

Assumptions listed above and the following were applied as well in the model:

- > In the stratification region, no conduction between the upper fire gas layer and the lower layer is assumed.
- > The mine drift is surrounded by homogeneous rock.
- > The initial temperature distribution in the rock mass is taken to be equivalent to the ambient temperature of the mine drift throughout.
- > The axial heat transfer is assumed to be negligible compared with the radial heat transfer.

For each time step and rock surface segment a number of parameters were calculated:

- > Convective heat transfer coefficient.
- > Energy balance of control volume and fire gas temperature.
- > Rock surface temperature.
- > Temperature of interior rock nodes.

Figures 4 and 5 display the calculation flow when calculating the convective heat transfer coefficient and increment in fire gas temperature for each rock surface segment and time step.

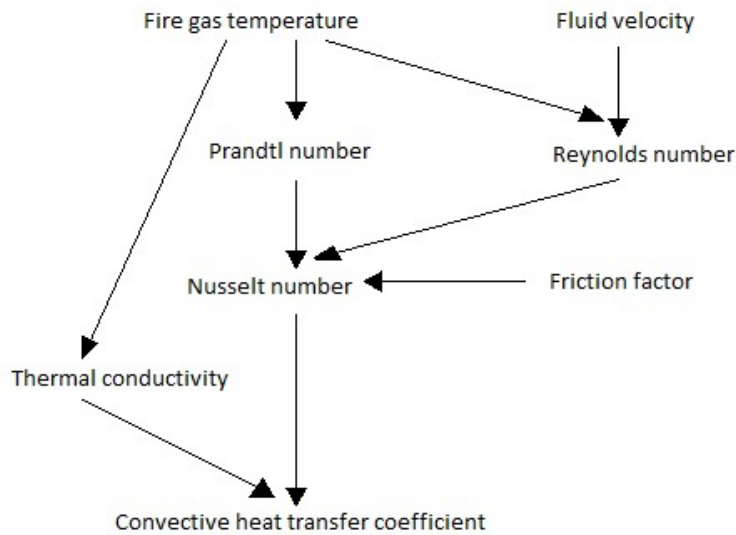
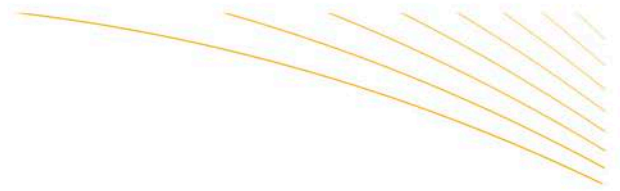


Figure 4. The calculation of the convective heat transfer coefficient

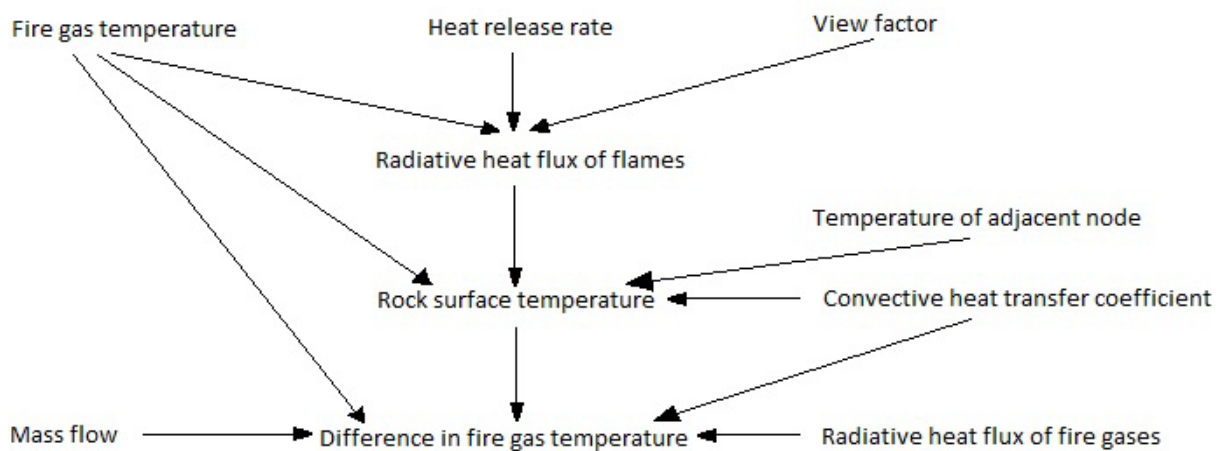


Figure 5. The calculation of the increase in the fire gas temperature

When calculating the convective heat transfer coefficient, the measured average fluid velocity from the experiments was used. The average fire gas temperature at the site of the fire was calculated using equation (6) and the heat release rates of the two experiments. The convective fraction of the total heat release rate may be assumed at 2/3 (Ingason et al., 1994) as an overall value. When applying equation (26) for calculating the average Nusselt number for the entry region, the distance  $x$  starts from the position of the fire as the velocity profile at that position is assumed to be fully developed.

The energy balance of a control volume of fire gases - where the boundary is the rock surface segment - was expressed by:



$$h_c \cdot (T_g - T_w) \cdot dA + \dot{q}_{rad}'' \Big|_{y=0} \cdot dA = \dot{m}_a \cdot c_p \cdot dT_g \quad (35)$$

The temperature difference -  $dT_g$  - was used when calculating the average gas temperature of the adjacent segment and time step. The radiative component in equation (35) will only contain the incident heat flux from the fire gases. The incident heat flux from the flames was accounted for when calculating the new temperature of the rock surface.

The solid boundary condition at a plane on the rock surface (equation (17) above) can be approximated by the following finite-difference approximation for a rock surface node 1 (setting the energy conducted, convected and radiated into the node equal to the increase in the internal energy of the node), applying a one-dimensional cylindrical system:

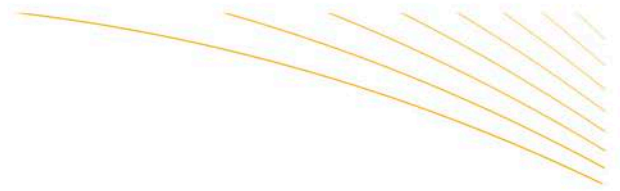
$$T_1^{i+1} = T_1^i + \frac{2 \cdot \Delta t}{\rho_s \cdot c_{p,s} \cdot (r_1 + 0.25 \cdot \Delta r) \cdot (\Delta r)^2} \cdot \left( -k \cdot (r_1 + 0.5 \cdot \Delta r) \cdot (T_2^i - T_1^i) + r_1 \cdot \Delta r \cdot \left( h \cdot (T_g - T_1^i) + \dot{q}_{rad}'' \Big|_{r=R} \right) \right) \quad (36)$$

In the calculations  $\Delta r = 0.1$  m was applied.

Similarly, the finite-difference approximation for an interior rock node  $m$  is given by:

$$T_m^{i+1} = T_m^i + \frac{\Delta t}{\rho_s \cdot c_{p,s} \cdot r_m \cdot (\Delta r)^2} \cdot \left( k \cdot \left( r_m + \frac{\Delta r}{2} \right) \cdot (T_{m+1}^i - T_m^i) + k \cdot \left( r_m - \frac{\Delta r}{2} \right) \cdot (T_{m-1}^i - T_m^i) \right) \quad (37)$$

Newman (1984) presented a correlation between the mass concentration of any chemical compound and the local gas temperature rise. Studying the fire gas temperature readings at the measuring station during the drilling rig and the loader fire, it was found that the thermocouple 4.3 m above the ground displayed consistently higher temperatures while the thermocouple 3.1 m above the ground displayed more or less ambient temperatures throughout the two experiments. As the distance between the fire and the measuring station was within region I with distinct stratification, the height of the fire gas layer was assumed to be in between the two thermocouples - i.e. 3.7 m above ground - throughout the experiments.



## 5. Results of experiments and three-dimensional analysis

The resulting average fire gas temperature curves of the various correlations were calculated and depicted together with the measured average fire gas temperature of the two full-scale experiments. See figures 4 to 15 for the resulting curves for the initial 20 minutes - encompassing the time period to the maximum heat release rate of both experiments. Equations (1) and (2) were also applied in the analysis, where equation (1) resulted in unrealistically high fire gas temperatures while equation (2) resulted in unrealistically low fire gas temperatures.

### 5.1 Drilling rig fire

When studying the average fire gas temperature curves of the drilling rig it can be seen that the correlation by Nunner (1956) - equation (22) - matched the measured values very well during the initial 20 minutes. It was only during the very last phase - as seen in figure 9 - that the correlation predicted much higher temperatures when comparing with the measured values. At this stage of the fire a backlayering started to occur.

The other correlations can be seen to significantly over predict the average fire gas temperature at the measuring station. During the initial five minutes the calculated results follows the measured results nicely, but then gradually the difference between the results increase more and more.

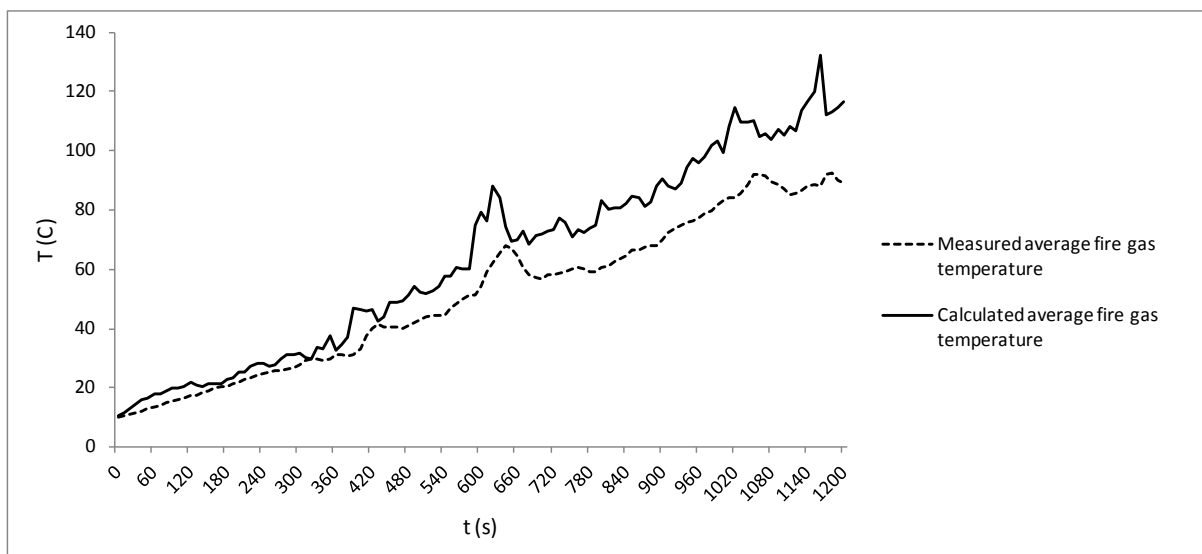


Figure 6. The measured and calculated - using equation (4) - average fire gas temperature in the case of the drilling rig fire

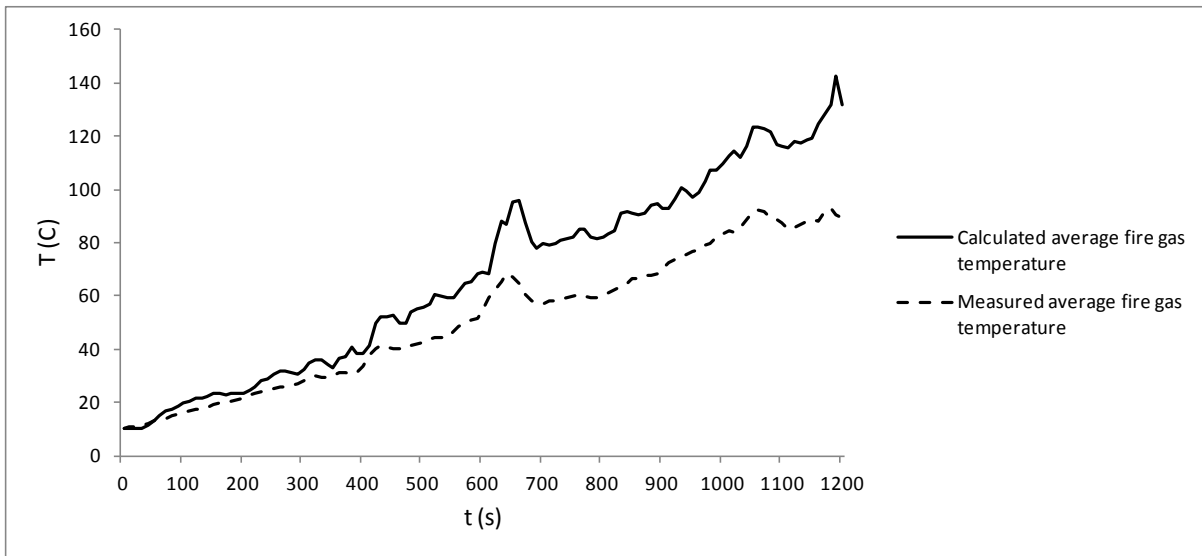


Figure 7. The measured and calculated - using equation (7) - average fire gas temperature in the case of the drilling rig fire

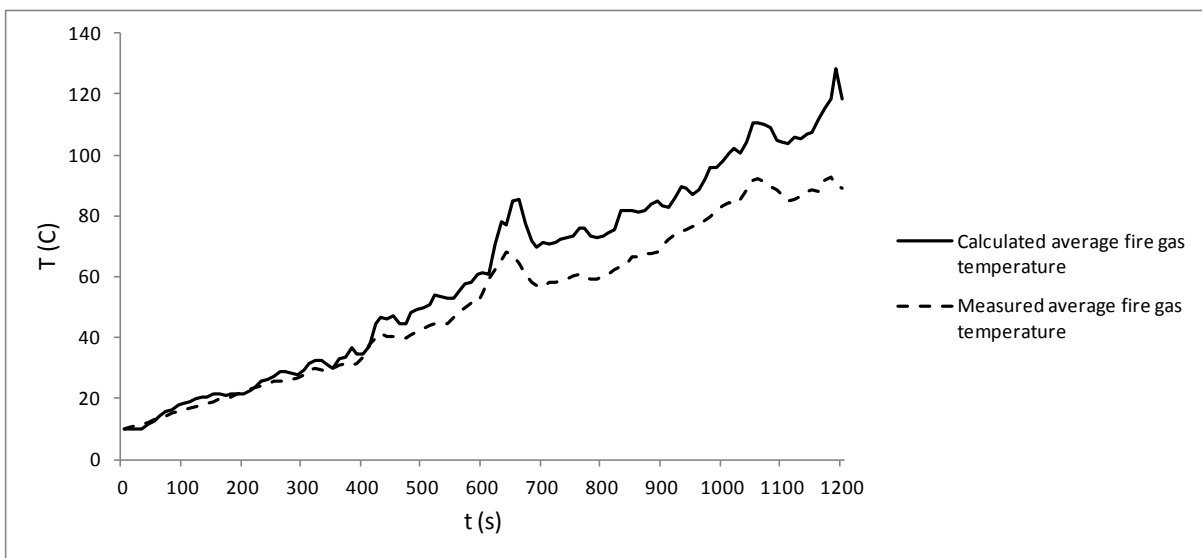


Figure 8. The measured and calculated - using equation (21) - average fire gas temperature in the case of the drilling rig fire

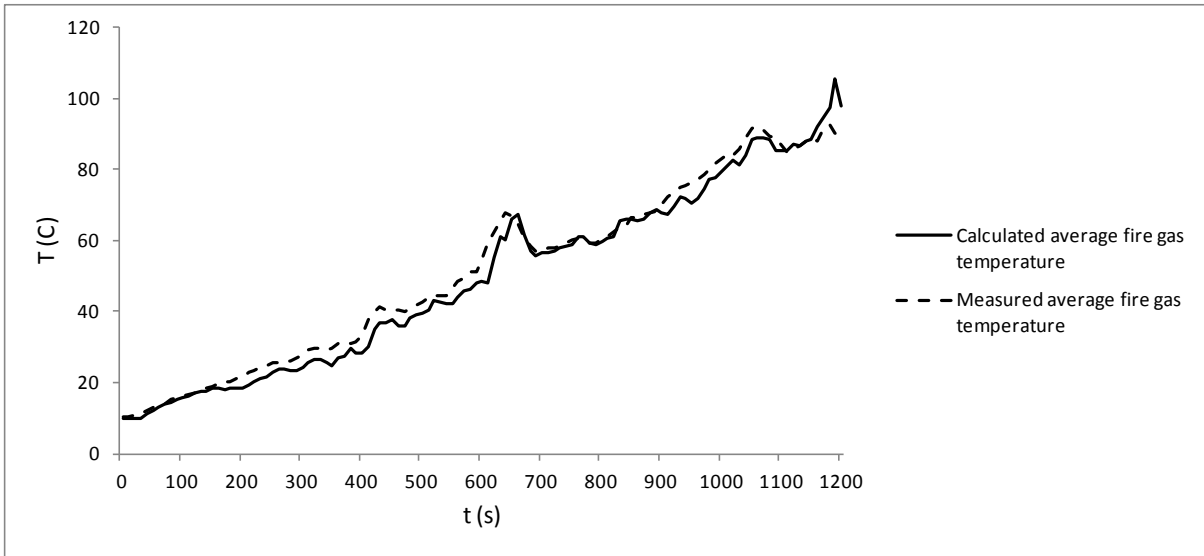
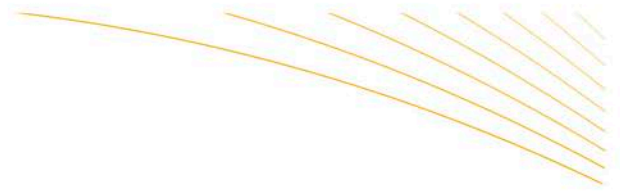


Figure 9. The measured and calculated - using equation (22) - average fire gas temperature in the case of the drilling rig fire

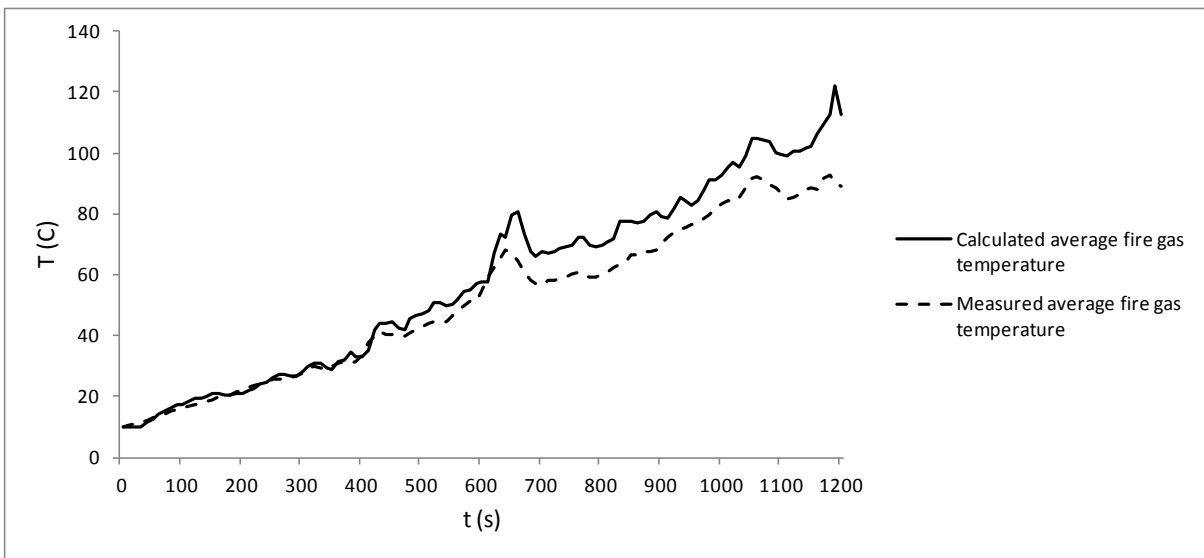


Figure 10. The measured and calculated - using equation (23) - average fire gas temperature in the case of the drilling rig fire

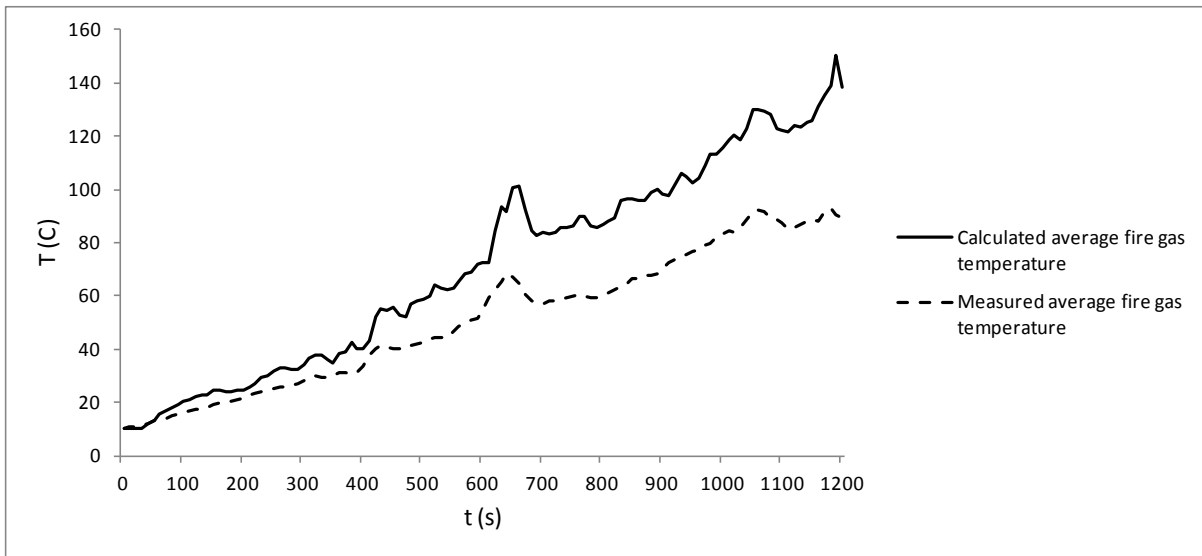


Figure 11. The measured and calculated - using equation (24) - average fire gas temperature in the case of the drilling rig fire

## 5.2 Loader fire

Same as for the drilling rig, the correlation by Nunner (1956) - equation (22) - matched the measured values very well during the initial 10 minutes. During the ensuing 10 minutes - as seen in figure 15 - the correlation predicted much higher temperatures when comparing with the measured values. At this stage of the fire a backlayering started to occur, resulting in a maximum backlayering of 50 m (Hansen and Ingason, 2013).

The other correlations can be seen to significantly over predict the average fire gas temperature at the measuring station.

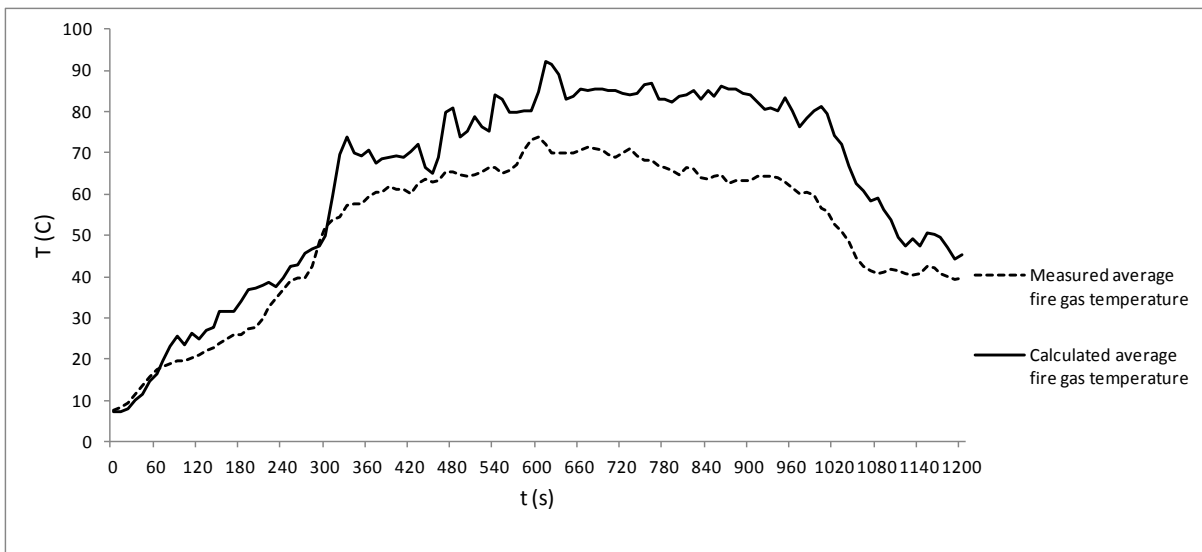


Figure 12. The measured and calculated - using equation (4) - average fire gas temperature in the case of the loader fire

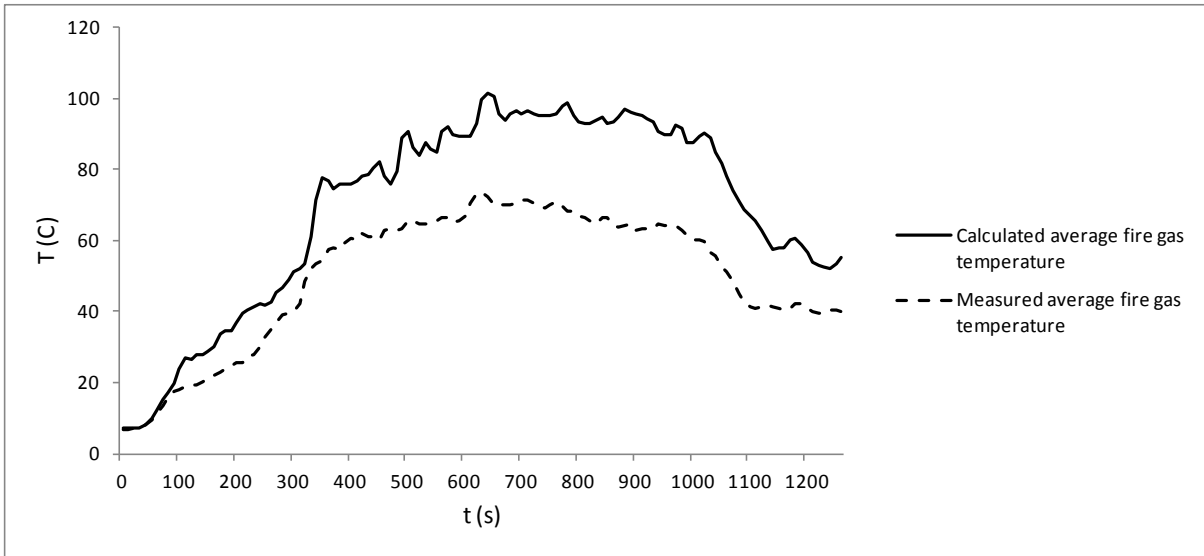
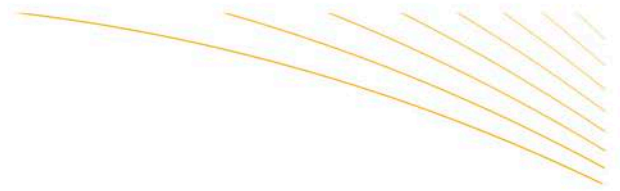


Figure 13. The measured and calculated - using equation (7) - average fire gas temperature in the case of the loader fire

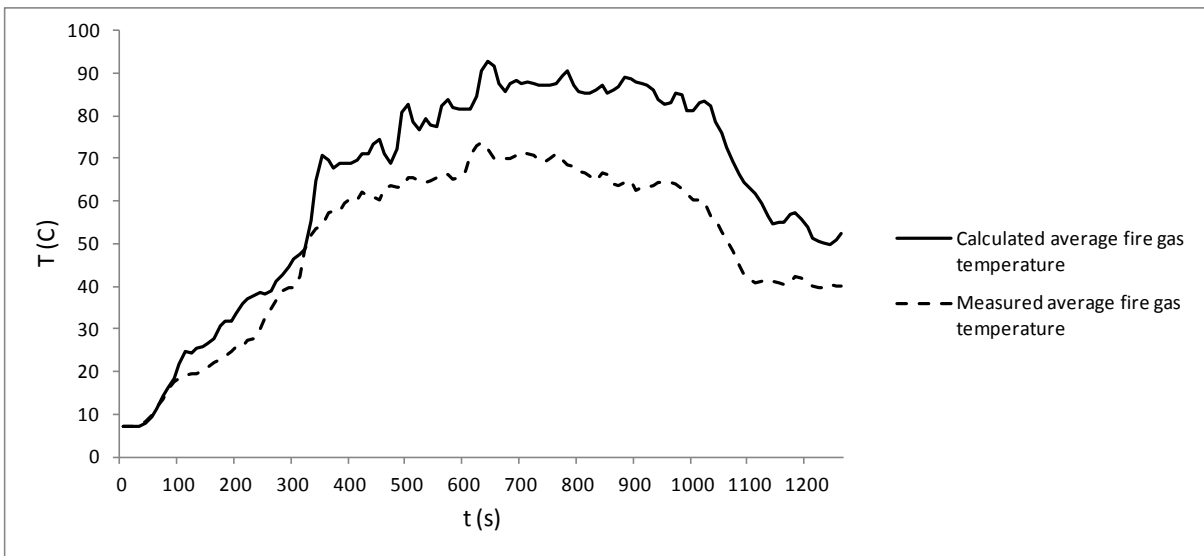


Figure 14. The measured and calculated - using equation (21) - average fire gas temperature in the case of the loader fire

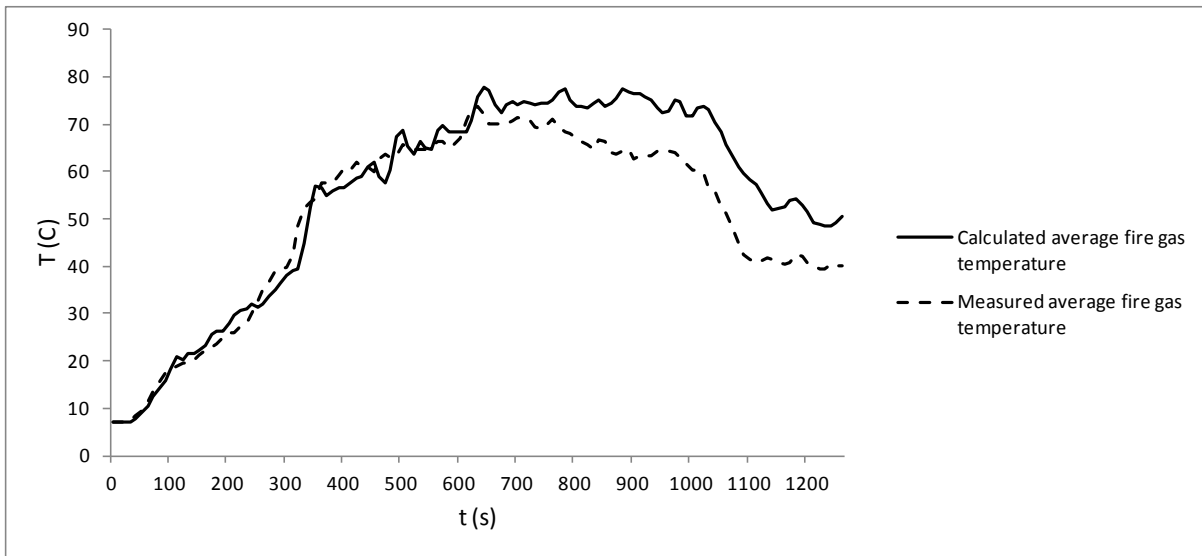


Figure 15. The measured and calculated - using equation (22) - average fire gas temperature in the case of the loader fire

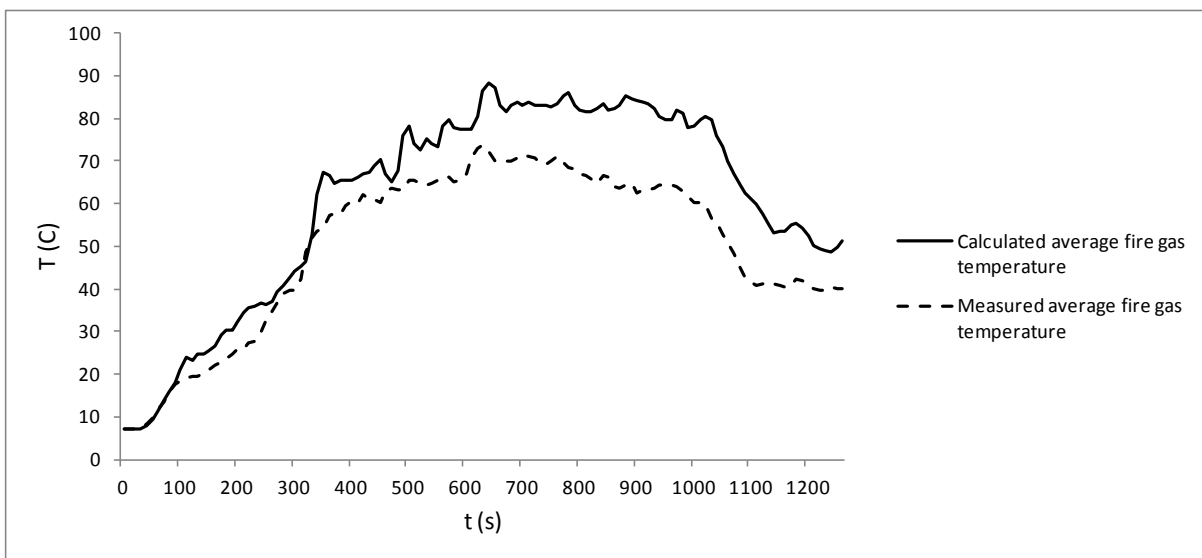


Figure 16. The measured and calculated - using equation (23) - average fire gas temperature in the case of the loader fire

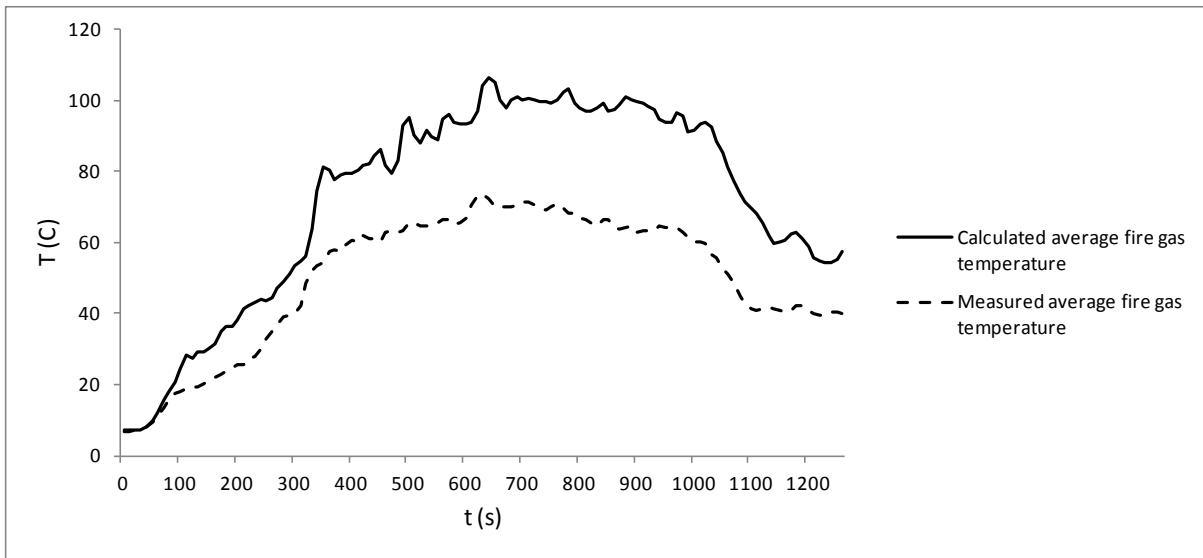
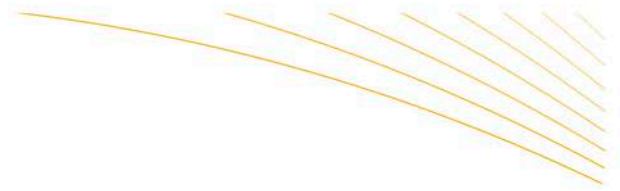


Figure 17. The measured and calculated - using equation (24) - average fire gas temperature in the case of the loader fire



## 6. Discussion

Equation (22) clearly fitted the measured results from the two experiments best among the investigated correlations. But a correlation accounting for the surface roughness will not necessarily predict the average fire gas temperature more accurate than a correlation that does not consider the surface roughness. As seen from the resulting graphs, equations (4) and (7) fitted the measured values better than equation (24) even though only the latter equation accounted for surface roughness.

The condition of equation (22) -  $Pr \approx 0.7$  - is valid for a wide temperature range which will imply a wide applicability of the equation for fires in mining drifts. Few fires in a mine would not fulfil this condition, if any fire at all.

The correlation by Nunner (1956) - equation (22) - matched the measured values very well during the initial 20 minutes of the drilling rig fire and the initial 10 minutes of the loader fire, a common denominator at these stages was the occurrence of the maximum heat release rate as well as backlayering. When backlayering occurred heat losses in the fire gases occurred upstream as well and the distance where losses occurred was therefore larger than the distance between the fire and the measuring station. The maximum backlayering in the case of the loader fire was 50 m, if assuming that the backlayering increased linearly (no recordings of the backlayering as a function of the time were taken during the experiments) with time starting at  $t=600$  s and subtracting the energy lost to backlayering at the various point of time from the heat release rate, the resulting temperature curve can be seen in figure 18. As noted the calculated average fire gas temperature fits the measured values very well.

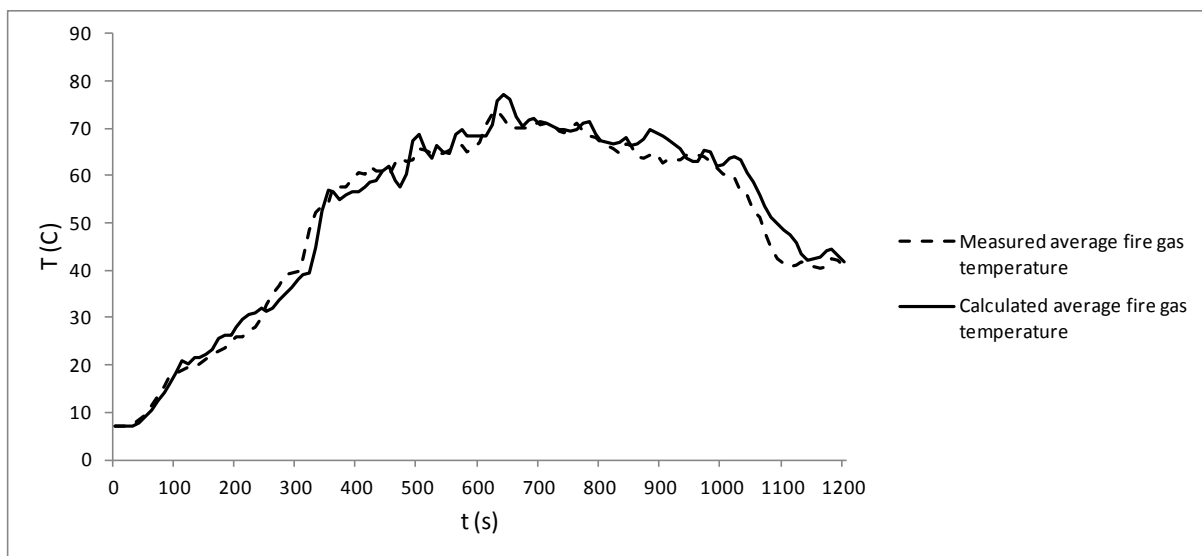
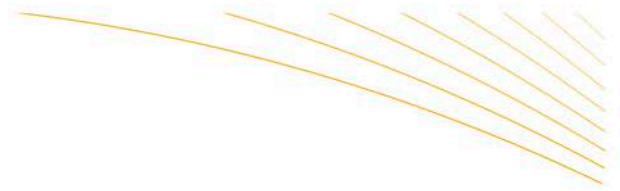


Figure 18. The measured and calculated - using equation (22) - average fire gas temperature in the case of the loader fire where the backlayering was accounted for

In the calculations of the analysis both the convective and the radiative heat transfer components were included. A question here is how much will the radiative component contribute to the average fire gas temperature. Calculations were performed where the radiative heat transfer component was set to zero in the case of the two experiments. Figure 19 displays the resulting average fire gas temperature of the loader using equation (22). As can be seen when comparing figure 15 and 19, the difference in the resulting average fire gas temperature is very small. The radiative heat transfer component could have been set to zero in the analysis and it would still not influence the resulting temperature. Clearly, the convective heat transfer component dominated over the radiative heat transfer component. However, the radiative heat transfer component cannot be entirely ruled out when analysing the risk of ignition of an adjacent object as the view factor will increase if an object is in parallel to the flames instead of perpendicular. An increase in



the view factor will result in a larger radiative component.

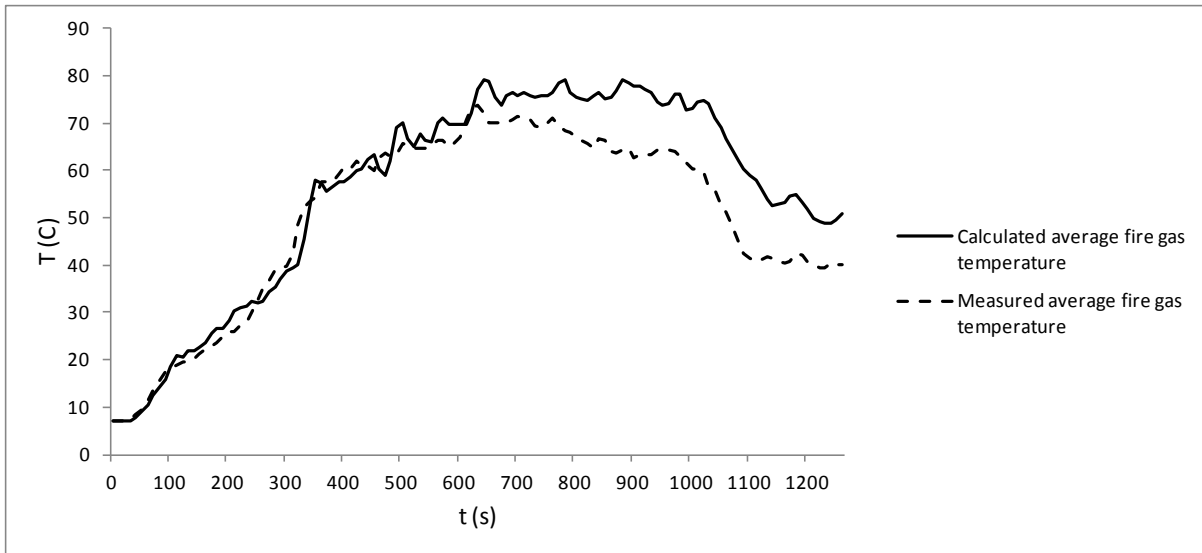


Figure 19. The measured and calculated - using equation (22) - average fire gas temperature in the case of the loader fire where the radiative component was set to zero

When applying the correlations that account for the surface roughness, the question arises whether a small change in the roughness amplitude will have a large effect on the resulting temperature. Applying equation (22) and using the roughness amplitude of 0.06 m and 0.14 m instead resulted in average fire gas temperatures found in figure 20 and 21 respectively. When comparing the results with the corresponding temperature curve found in figure 9 it can be seen that the temperature difference is fairly small between the different cases. Thus equation (22) will not be very sensitive to changes in the roughness amplitude and the measurement of the roughness amplitude in a mine drift may not have to be exact.

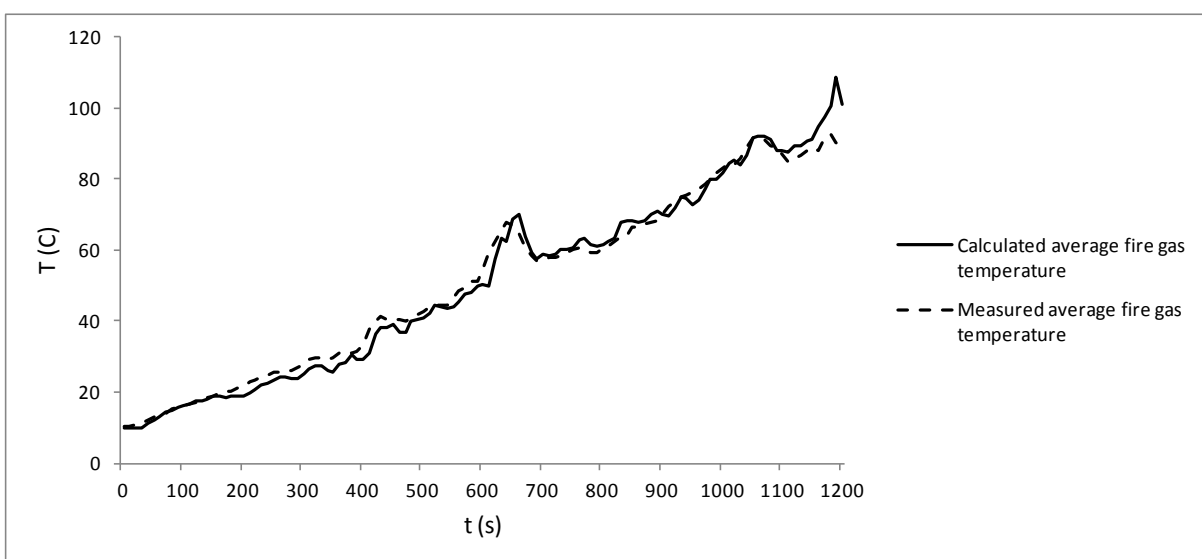


Figure 20. The measured and calculated - using equation (22) - average fire gas temperature in the case of the drilling rig fire where the roughness amplitude was set to 0.06 m

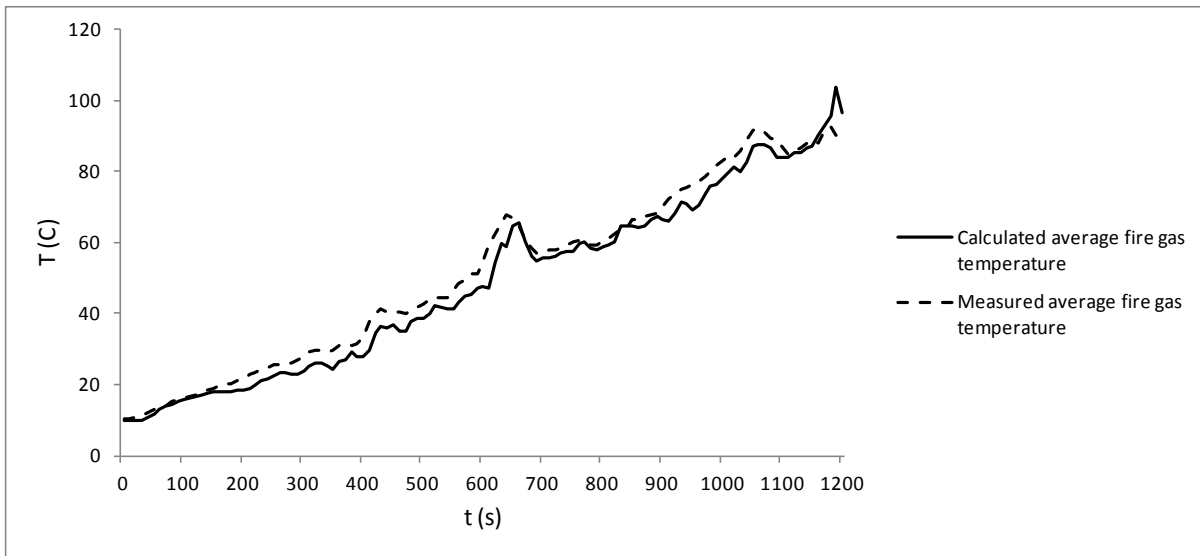


Figure 21. The measured and calculated - using equation (22) - average fire gas temperature in the case of the drilling rig fire where the roughness amplitude was set to 0.14 m

The rock surface temperature will increase due to the heat transfer from the flames and the fire gases. The question is how much will the temperature increase and would it have to be included in the calculations? When studying the calculated rock surface temperatures of the two experiments it was found that the temperature increase at the site of the fire was more than 100 degrees after approximately 20 minutes. Further 20 m downstream of the fire the temperature increase was approximately 25 degrees. The temperature increase is considerable and will have to be taken into account during the calculations. A longer lasting fire would have increased the rock surface temperature even more, underlining the importance of including the heat transfer calculations to the surrounding rock surface.

The temperature change in the x-direction of the solid was examined and found to be small compared with the temperature change in the radial direction. Thus the assumption that the axial heat transfer would be negligible compared with the radial heat transfer was found to be valid.

Calculations were also performed where the fully developed case was applied instead of the entry region case. Resulting average fire gas temperatures were significantly lower than the measured temperatures and the entry region condition will have to be applied.

During the analysis the height of the fire gas layer was set to 3.7 m above ground, based upon the temperature readings of the thermocouples at the measuring station. In many situations there may not be any data available when pinpointing the height of the fire gas layer, the question then arises how sensitive the output is to a change in the layer height? If instead assuming that the fire gas layer was approximately mid-height and lowering the layer height by 1 meter to 2.7 m, would that have had a significant effect on the resulting temperature? Calculations were performed where the height of the fire gas layer was lowered respectively raised by 1 meter. In figure 22 the resulting average fire gas layer temperature when raising the layer height by 1 meter can be found for the drilling rig fire. As can be seen, the 1 meter difference in fire gas layer height did not have a significant impact on the resulting temperature. Similar temperature differences were found when lowering the layer height by 1 meter.

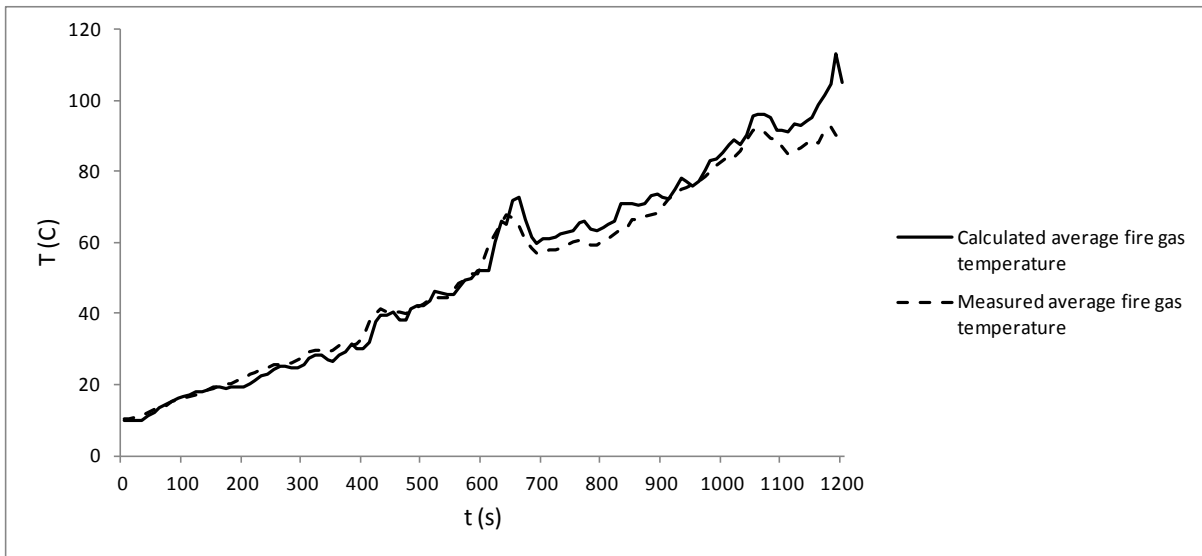
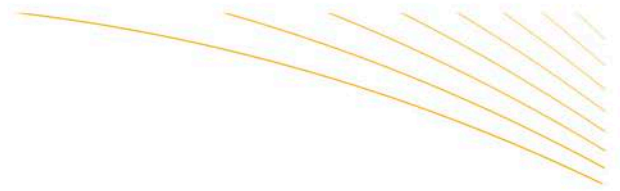


Figure 22. The measured and calculated - using equation (22) - average fire gas temperature of the drilling rig when raising the layer height by 1 meter

In order to further validate the correlation by Nunner and the presented model, fire experiments should be performed where the average fire gas temperature is measured closer to the fire source in order to obtain higher gas temperatures that are applicable for fire spread analysis. The average fire gas temperatures should also be measured at positions further downstream of the fire in order to validate correlation and model for fully developed turbulent flow conditions.

Knowing the average fire gas temperature will be a key factor when analyzing the smoke behaviour and designing the egress safety of the area in question as well as the smoke control. Knowing the average fire gas temperature will also be a key factor when determining the risk of fire spread to adjacent items, setting up safety distances to prevent ignition of multiple objects etc. It is important to point out that the average fire gas temperatures measured and calculated in this paper were relatively low and would not have posed any significant risk with respect to fire spread. Knowing the average fire gas temperature will limit the impact on the surroundings and will increase the safety of the miners as well as fire personnel.

As seen from the temperature results the rough rock surface in a mine drift will increase the heat losses of the fire gases compared with for example a tunnel with smooth surface. This in turn will decrease the risk of a flashover or a severe fire behaviour in a mine drift as the energy of the fire gases will not be sufficient. The open nature of a mine drift will decrease the risk even further, as fire gases will not be accumulated as in an enclosure.



## 7. Conclusions

---

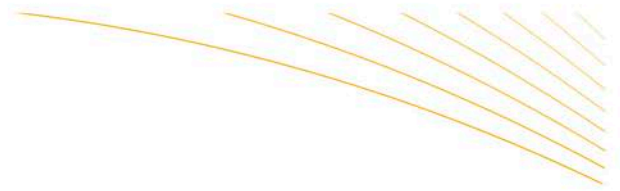
An analysis on the heat losses of fire gases in a mine drift with longitudinal ventilation was conducted, based upon two earlier full-scale fire experiments in a mine drift and a number of correlations for calculating the convective heat transfer coefficient or the average fire gas temperature directly. It is found that an expression by Nunner (1956) resulted in predicted average fire gas temperatures closest to the corresponding temperatures of the two experiments. The other correlations are found to significantly over predict the average fire gas temperature.

It was only during the later phases that the correlation by Nunner predicted much higher temperatures when comparing with the measured values. A common denominator at these stages was the occurrence of the maximum heat release rate as well as backlayering. When subtracting the energy lost to backlayering at the various point of time from the heat release rate, the resulting calculated temperature curve was found to fit the measured values very well.

A sensitivity analysis showed that the difference in the resulting average fire gas temperature is very small if the radiative heat transfer component was set to zero. This indicated that the convective heat transfer component dominated over the radiative heat transfer component at the position of the measuring station - approximately 35 m downstream of the loader fire and 50 m downstream of the drilling rig fire. Two other sensitivity analyses showed that the correlation by Nunner is not very sensitive to changes in the roughness amplitude or the height of the fire gas layer and the measurement of the parameters in a mine drift may be estimated and not determined exactly.

The rock surface temperature was found to increase at the site of the fire more than 100 degrees after approximately 20 minutes from the start of the fire. Further downstream of the fire the temperature increase was also found to be considerable and therefore the temperature increase will have to be taken into account during the calculations and cannot be neglected.

A fire in an underground mine will always pose a risk. But if knowing the average fire gas temperature, the smoke behaviour in an area could be analysed and appropriate measures could be taken with respect to the egress safety and the smoke control. This will increase the safety of the miners as well as the fire personnel.



## 8. References

---

- Beard A. et al. (2005) The handbook of tunnel fire safety. London: Thomas Telford Ltd.
- Bhatti MS, Shah RK. (1987) Turbulent and Transition Flow Convective Heat Transfer in Ducts. In: Kakaç S, Shah RK, Aung W, editors. Handbook of single-phase convective heat transfer: Wiley-Interscience.
- Chang X, Greuer RE. (1985) Simplified method to calculate the heat transfer between mine air and mine rock. Proceedings of the 2<sup>nd</sup> US Mine Ventilation Symposium 1985:429-438.
- Chang X, Greuer R. (1987) A mathematical model for mine fires. Proceedings of the 3<sup>rd</sup> Mine Ventilation Symposium 1987:453-462.
- Chung BTF, Sumitra PS. (1972) Radiation shape factors from plane point sources. Journal of Heat Transfer 1972;94:328-330.
- Dziurzynski W, Tracz J, Trutwin W. (1988) Simulation of mine fires. 4<sup>th</sup> International Mine Ventilation Congress, Brisbane.
- Hansen R, Ingason H. (2013) Heat Release Rate Measurements of Burning Mining Vehicles in an Underground Mine. Fire Safety Journal 2013;61:12-25.
- Hansen R. (2015) Study of heat release rates of mining vehicles in underground hard rock mines. Doctoral thesis. Västerås: Mälardalen University.
- Hansen R. (2015) Analysis of Methodologies for Calculating the Heat Release Rates of Mining Vehicle Fires in Underground Mines. Fire Safety Journal 2015;71:194-216.
- Hottel HC. (1954) Radiant Heat Transmission. In: McAdams WH, editor. Heat Transmission, New York: McGraw-Hill.
- Incropera FP, Dewitt DP, Bergman TL, Lavine AS. (2007) Fundamentals of Heat and Mass Transfer. Hoboken: John Wiley & Sons Inc.
- Ingason H, Gustavsson S, Dahlberg M. (1994) Heat release rate measurements in tunnel fires. Borås: SP report 1994:08.
- Ingason H, Li YZ. (2010) Model scale tunnel fire tests with longitudinal ventilation. Fire Safety Journal 2010;45:371-384.
- Martinelli RC. (1947) Heat Transfer to Molten Metals. Trans. ASME 1947;69:947-959.
- McPherson MJ. (1986) The analysis and simulation of heat flow into underground airways. International Journal of Mining and Geological Engineering. 1986;4:165-196.
- Mills AF. (1962) Experimental Investigation of Turbulent Heat Transfer in the Entrance Region of a Circular Conduit. J. Mech. Eng. Sci. 1962;4:63-77.
- Newman JS. (1984) Experimental Evaluation of Fire-Induced Stratification. Combustion and Flame 1984;57:33-39.
- Newman JS, Tewarson A. (1983) Flame Propagation in Ducts. Combustion and Flame 1983;51:347-355.
- Norris RH. (1970) Some Simple Approximate Heat-Transfer Correlations for Turbulent Flow in Ducts with Rough Surfaces. In: Bergles AE, Webb RL, editors. Augmentation of Convective Heat and Mass Transfer, New York: The Winter Annual Meeting of the American Society of Mechanical Engineers.
- Nunner W. (1956) Wärmeübergang und Druckabfall in Rauhen Rohren. VDI-Forschungsheft 445, Ser. B 1956;22:5-39.



Rohsenow WM, Choi HY. (1963) Heat, mass and momentum transfer. Prentice-Hall Inc.

Scott DR. (1958) The cooling of underground galleries. Transactions of the Institution of Mining Engineers 1958;118:356-372.

Simode E. (1985) Simulation of thermal and aerodynamic effects of a fire in a complex underground ventilation network. Proceedings of the 2<sup>nd</sup> US Mine Ventilation Symposium 1985:455-459.

Starfield AM, Dickson AJ. (1967) A study of heat transfer and moisture pick-up in mine airways. Journal of the South African Institute of Mining and Metallurgy, 1967;68:211-234.

Wilson JS. (2004) Sensor technology handbook. Elsevier.

Wolski JK. (1995) Modeling of heat exchange between flowing air and tunnel walls. Proceedings of the 7<sup>th</sup> US Mine Ventilation Symposium 1995:207-212.